

Synthetical optimization of the structure dimension for the thermoacoustic regenerator

Huifang Kang(康慧芳), Lingxiao Zhang(张凌霄), Jun Shen(沈俊),Xiachen Ding(丁夏琛), Zhenxing Li(李振兴), and Jun Liu(刘俊)

Citation: Chin. Phys. B, 2022, 31 (**3**): 034301. DOI: 10.1088/1674-1056/ac1f02
Journal homepage: http://cpb.iphy.ac.cn; http://iopscience.iop.org/cpb

What follows is a list of articles you may be interested in

Deep learning for image reconstruction in thermoacoustic tomography

Qiwen Xu(徐启文), Zhu Zheng(郑铸), and Huabei Jiang(蒋华北)
Chin. Phys. B, 2022, 31 (**2**): 024302. DOI: 10.1088/1674-1056/ac0dab

Thermoacoustic assessment of hematocrit changes in human forearms

Xue Wang(王雪), Rui Zhao(赵芮), Yi-Tong Peng(彭亦童), Zi-Hui Chi(迟子惠), Zhu Zheng(郑铸), En Li(李恩), Lin Huang(黄林), and Hua-Bei Jiang(蒋华北)
Chin. Phys. B, 2021, 30 (**9**): 094302. DOI: 10.1088/1674-1056/ac041c

Influence exerted by bone-containing target body on thermoacoustic imaging with current injection

Yan-Hong Li(李艳红), Guo-Qiang Liu(刘国强), Jia-Xiang Song(宋佳祥), Hui Xia(夏慧)
Chin. Phys. B, 2019, 28 (**4**): 044302. DOI: 10.1088/1674-1056/28/4/044302

Thermoacoustic-reflected focusing lens based on acoustic Bessel-like beam with phase manipulation

An-Ru Hou(侯安茹), Wen-Ting Gao(高文婷), Jiao Qian(钱姣), Hong-Xiang Sun(孙宏祥), Yong Ge(葛勇), Shou-Qi Yuan(袁寿其), Qiao-Rui Si(司乔瑞), Xiao-Jun Liu(刘晓峻)
Chin. Phys. B, 2018, 27 (**12**): 124301. DOI: 10.1088/1674-1056/27/12/124301

Nonlinear impedances of thermoacoustic stacks with ordered and disordered structures

Ge Huan, Fan Li, Xia Jie, Zhang Shu-Yi, Tao Sha, Yang Yue-Tao, Zhang Hui
Chin. Phys. B, 2014, 23 (**7**): 074301. DOI: 10.1088/1674-1056/23/7/074301

Synthetical optimization of the structure dimension for the thermoacoustic regenerator

Huifang Kang(康慧芳)[1,†], Lingxiao Zhang(张凌霄)[1], Jun Shen(沈俊)[2], Xiachen Ding(丁夏琛)[1], Zhenxing Li(李振兴)[2], and Jun Liu(刘俊)[1]

[1] *Beijing Institute of Technology, Beijing* 100124, *China*

[2] *Technical Institute of Physics and Chemistry, Chinese Academy of Sciences, Beijing* 100190, *China*

(Received 6 May 2021; revised manuscript received 14 July 2021; accepted manuscript online 19 August 2021)

The quantitative investigation of parameters in the renegerator is essential for the optimization of thermoacoustic devices, while the majority of the previous research only considered parameters of the working field, working gas and the hydraulic radius. Based on the linear thermoacoustic theory, this paper extracts a normalized parameter for low-amplitude conditions, which is called the regenerator operation factor. By extracting the regenerator operation factor and relative hydraulic radius, the influence of frequency on the efficiency can be controlled and offset. It can be found that thermoacoustic devices with different frequencies can perform the same efficiency by adjusting the radius in proportion to the axial length. Finally, this paper synthetically optimizes the dimension of the thermoacoustic regenerator by taking the regenerator operation factor, relative hydraulic radius and acoustic field parameter as variables. Conclusions in this paper are of great significance for explaining the best working conditions of engines and directing the miniaturization and optimal design of thermoacoustic devices.

Keywords: thermoacoustic, regenerator, hydraulic radius, regenerator length

PACS: 43.20.+g, 43.35.Ud, 44.30.+v **DOI:** 10.1088/1674-1056/ac1f02

1. Introduction

Due to thermoacoustic effects, the thermoacoustic engine (TAE) can convert the heat to the acoustic wave, and the thermoacoustic cooler (TAC) can also pump heat through the acoustic wave. The regenerator for thermoacoustic conversions is the core of the thermoacoustic devices. In the TAE, acoustic waves are triggered when a steep temperature gradient is established along the regenerator. Acoustic waves cause gas parcels in the regenerator to go through a thermodynamic cycle consisting of compression, heating, expansion and cooling processes. As a result, the conversion process from heat to acoustic energy does not have any moving parts.[1] In the TAC, when the acoustic wave passes through the regenerator, a temperature gradient along the regenerator with a certain coefficient of performance (COP) is established. Gas parcels affected by acoustic waves in the regenerator undergo the thermodynamic cycle consisting of compression, cooling, expansion and heating processes. Thus, moving parts are not required in the heat pumping process,[2] as well.

In 1962, Carter[3] enhanced the thermoacoustic effects by inserting a regenerator into the Sondhauss tube[4] and stimulated the investigation of the thermoacoustic regenerator function. In 1979, Ceperley[5] firstly described the thermoacoustic regenerator as an energy conversion apparatus, and experimentally testified the thermoacoustic conversion function. Fundamentals of physical principles underlying the regenerator were investigated and analyzed in previous papers,[6,7] while the regenerator's parameters were optimized by several researchers.[7–12]

Swift[7] studied the hydraulic radius r_h in the thermoacoustic system and obtained the empirical values: $r_h/\delta_k \sim 1$ for standing wave engine and $r_h/\delta_k \ll 1$ for traveling wave engine, where δ_k is the thermal penetration depth. Tijani[8] studied a standing wave thermoacoustic cooler and put forward that $r_h = 1.25\delta_k$ was optimal for the cooling power, $r_h = 2.0\delta_k$ led to the lowest temperature, and the highest efficiency could be reached when $r_h = 1.5\delta_k$. Yu[9] found that a measured optimal value was $r_h \approx (0.3 \sim 0.2)\delta_v$ for the excitation of the system with the viscous penetration depth δ_v in a traveling wave thermoacoustic engine. Raspet[10] presented the correlation of the coefficient of performance of the thermoacoustic cooler with the standing wave ratio and optimized the regenerator structure by adjusting the standing wave ratio. Tijani[11] experimentally investigated the effect of Prandtl number on the performance of a thermoacoustic refrigerator using gas mixtures. Kazuto[12] considered correlations of the local Nusselt number distribution and analyzed heat transfer characteristics of the oscillatory flow in the engine core via numerical simulations.

However, those publications[7–12] were unilateral to understand the optimal condition for the thermoacoustic conversion. Most of those regenerator optimizations[7–12] analyzed parameters of the working field, working gas and the hydraulic radius, whereas the quantitative investigation of important pa-

†Corresponding author. E-mail: kanghf@bit.edu.cn

© 2022 Chinese Physical Society and IOP Publishing Ltd

rameters, for example, the length of the regenerator, on the behavior of thermoacoustic devices was still lacking. In the previous design,[13–25] the selection of the regenerator length was dependent on the experience, which caused the design with some blindness and results without prescient considerations, as well as the limited performance rather than the optimal.

Thus, this paper presents a normalized parameter, the regenerator operation factor, based on the linear thermoacoustic theory for the small-amplitude condition without the nonlinear linearity involved. The influence of frequency on efficiency can be controlled and offset manually, while the thermoacoustic devices with various frequencies can perform the same efficiency. This is of significance to guide the miniaturization design of the thermoacoustic device. Moreover, by extracting and analyzing the regenerator operation factor in the basic thermoacoustic formulas, the parameters relative to the regenerator length are obtained and can be used to optimize the regenerator length. Finally, this paper synthetically optimizes the structure dimension of the thermoacoustic regenerator by combining the regenerator operation factor, relative hydraulic radius and acoustic field parameter.

2. Thermoacoustic formula extracting

2.1. Heat flow

In the thermoacoustic regenerator model, ordinary thermal conduction in direction is neglectable. The time-averaged heat flow generated across regenerator due to the hydrodynamics transport is[26,27]

$$\dot{Q} = \int \left[\rho_{\mathrm{m}} c_{\mathrm{p}} \mathrm{Re}[T_1 \tilde{u}_1] - \mathrm{Re}[p_1 \tilde{u}_1]\right] \mathrm{d}A, \tag{1}$$

where Re[ ] indicates the real part, the tilde indicates complex conjugation, A is the cross area of fluid, ρ_{m} is the mean density of the working gas, c_{p} is the isobaric specific heat per unit mass, p_1 is the oscillating pressure, T_1 is the oscillating temperature, u_1 is the oscillating velocity, and the expressions of T_1 and u_1 are as follows:[21]

$$T_1 = \frac{1}{\rho_{\mathrm{m}} c_{\mathrm{p}}} (1-h_k)\, p_1 - \frac{1}{\mathrm{i}\omega} \frac{\mathrm{d}T_{\mathrm{m}}}{\mathrm{d}x} \frac{(1-h_k)-\sigma(1-h_v)}{(1-\sigma)(1-f_v)} u_1, \tag{2}$$

$$u_1 = \frac{\mathrm{i}}{\omega \rho_{\mathrm{m}}} \frac{\mathrm{d}T_{\mathrm{m}}}{\mathrm{d}x} (1-h_k) \frac{\mathrm{d}p_1}{\mathrm{d}x}, \tag{3}$$

while T_{m} is the mean temperature, ω is the angular frequency, σ is the Prandtl number, and h_v and h_k are the Rott's functions, which depend on the specific channel geometry under consideration.

According to Eqs. (1)–(3), the expression of the time-averaged heat flow can be yielded

$$\dot{Q} = \frac{|U_1|^2 \rho_{\mathrm{m}} c_{\mathrm{p}}}{2A\omega(1-\sigma^2)|1-f_v|^2} \frac{\mathrm{d}T_{\mathrm{m}}}{\mathrm{d}x} \mathrm{Im}\left(f_k + \sigma \tilde{f}_v\right) - \frac{1}{2} \mathrm{Re}\left[p_1 \tilde{U}_1 \left(\frac{f_k - \tilde{f}_v}{(1+\sigma)(1-\tilde{f}_v)}\right)\right], \tag{4}$$

where Im[ ] indicates the image part, U_1 is the volume flow rate, f_v and f_k are the spatially averaged Rott's functions, which also depend on the specific channel geometry under consideration.

Expressions of f_v and f_k are known for most geometries[26] and the solutions for most of these geometries are actually very similar. Therefore, this paper only takes the parallel plate-type regenerator as a case, and other types of regenerators can be analyzed in the similar way. The $y = 0$ is defined at the centerline of the spacing between two adjacent parallel plates

$$f_v = \frac{\tanh[(1+\mathrm{i})\, y_0/\delta_{\mathrm{v}}]}{(1+\mathrm{i})\, y_0/\delta_{\mathrm{v}}}, \tag{5}$$

$$f_k = \frac{\tanh[(1+\mathrm{i})\, y_0/\delta_k]}{(1+\mathrm{i})\, y_0/\delta_k}, \tag{6}$$

where $2y_0$ equals the thickness of each spacing and $r_{\mathrm{h}} = y_0$.

The relative hydraulic radius is the ratio of the hydraulic radius r_{h} to the thermal penetration depth δ_k, and is defined as $\zeta = r_{\mathrm{h}}/\delta_k$. Expressions of f_v and f_k can be written as follows:

$$f_v = \frac{\tanh\left[(1+\mathrm{i})\,\zeta\sqrt{1/\sigma}\right]}{(1+\mathrm{i})\,\zeta\sqrt{1/\sigma}}, \tag{7}$$

$$f_k = \frac{\tanh[(1+\mathrm{i})\,\zeta]}{(1+\mathrm{i})\,\zeta}. \tag{8}$$

For simple analysis, the time-averaged heat flow can be written as

$$\dot{Q} = \left(\frac{1}{2}|p_1||U_1|\right)\left[\frac{-\psi}{|Z_{\mathrm{N}}||1-f_v|^2(1-\sigma^2)(\gamma-1)} \times \mathrm{Im}\left(f_k + \sigma\tilde{f}_v\right) + \mathrm{Re}\left[\frac{f_k - \tilde{f}_v}{(1+\sigma)(1-\tilde{f}_v)} \mathrm{e}^{\mathrm{i}\varphi_Z}\right]\right], \tag{9}$$

where γ is the ratio of isobaric specific heat to isochoric specific heat, Z_{N} is the normalized impedance, φ_Z is the phase of Z_{N} and represents the leading phase of p_1 to u_1, and

$$Z_{\mathrm{N}} = \frac{p_1/u_1}{\rho_{\mathrm{m}} c} = |Z_{\mathrm{N}}|\, \mathrm{e}^{\mathrm{i}\varphi_Z}. \tag{10}$$

The ψ is the regenerator operation factor, which is derived from the basic thermoacoustic formulas and reflects the human-operable factor in the regenerator, including not only the structure dimension (e.g., l_{N}), but also the operation parameter (e.g., T_{h}). By extracting and analyzing the regenerator operation factor in the basic thermoacoustic formulas, the parameters relative to the regenerator length are obtained, and ψ is defined as

$$\psi = \frac{c}{\omega} \frac{1}{T_{\mathrm{m}}} \frac{\mathrm{d}T_{\mathrm{m}}}{\mathrm{d}x} = \frac{\lambda}{2\pi T_{\mathrm{m}}} \frac{\mathrm{d}T_{\mathrm{m}}}{\mathrm{d}x} \approx \frac{1}{\pi l_{\mathrm{N}}} \frac{T_{\mathrm{h}} - T_{\mathrm{c}}}{T_{\mathrm{h}} + T_{\mathrm{c}}}, \tag{11}$$

where $l_{\rm N}$ is the normalized length of the regenerator and is defined as $l_{\rm N}=l_{\rm reg}/\lambda$, the ratio of the length of the regenerator $l_{\rm reg}$ to the wavelength λ, $T_{\rm h}$ is the temperature of the hot end, and $T_{\rm c}$ is the temperature of the cool end.

2.2. Acoustic power

The average acoustic power $\mathrm{d}\dot{E}_2$ produced in a length $\mathrm{d}x$ of the regenerator is expressed as[27]

$$\frac{\mathrm{d}\dot{E}_2}{\mathrm{d}x}=-\frac{1}{2}\frac{\omega\rho_{\rm m}}{A}\frac{\mathrm{Im}\left[-f_v\right]}{\left|1-f_v\right|^2}\left|U_1\right|^2-\frac{1}{2}\frac{\gamma-1}{\gamma}\frac{\omega A\,\mathrm{Im}\left[-f_k\right]}{p_{\rm m}}\left|\tilde{p}_1\right|^2+\frac{1}{2}\frac{1}{T_{\rm m}}\frac{\mathrm{d}T_{\rm m}}{\mathrm{d}x}\mathrm{Re}\left[\frac{f_k-f_v}{(1-f_v)(1-\sigma)}\tilde{p}_1U_1\right],\tag{12}$$

where $p_{\rm m}$ is the mean pressure of the fluid.

The first two terms in Eq. (12) are always negative because they have no concern with the temperature gradient along x and describe the consumption of the acoustic power. The first term describes the viscous dissipation of the acoustic wave. It is proportional to $|u_1|^2$ and independent of thermal conductivity. The second term describes the thermal-relaxation dissipation and is proportional to $|p_1|^2$ and independent of viscosity. The third term is called the source term as it describes not only the production but also the consumption of acoustic power. Only if $\mathrm{d}T_{\rm m}/\mathrm{d}x\neq 0$ will the last term exist. As shown in Eq. (12), there are two means to produce more acoustic power: one is to reduce the viscous and thermal-relaxation dissipation, while the other is to increase the newly produced acoustic power.

For simple analysis, the average acoustic power gain can be written as

$$\frac{\mathrm{d}\dot{E}_2}{\mathrm{d}x}=\left(\frac{1}{2}\left|p_1\right|\left|U_1\right|\right)\left(\frac{1}{T_{\rm m}}\frac{\mathrm{d}T_{\rm m}}{\mathrm{d}x}\right)\times\left\{\frac{1}{\psi}\left[-\frac{\mathrm{Im}\left[-f_v\right]}{\left|1-f_v\right|^2}\times\frac{1}{|Z_{\rm N}|}-(\gamma-1)\,\mathrm{Im}\left[-f_k\right]\times|Z_{\rm N}|\right]+\mathrm{Re}\left[\frac{f_k-f_v}{(1-f_v)(1-\sigma)}\,\mathrm{e}^{-\mathrm{i}\varphi_Z}\right]\right\}.\tag{13}$$

2.3. Second law efficiency of the TAE

The first law efficiency η_1 divided by the Carnot efficiency $\eta_{\rm c}$ equals the second law efficiency η_2, that is,

$$\eta_2=\eta_1/\eta_{\rm c}.\tag{14}$$

According to Eqs. (9), (13) and (14), it can be yielded

$$\eta_2=\frac{\eta_1}{\eta_{\rm c}}=\frac{\Delta\dot{E}_2/\dot{Q}_{\rm h}}{\Delta T_{\rm m}/T_{\rm m}}=\frac{\frac{\mathrm{d}\dot{E}_2/\mathrm{d}x}{\dot{Q}_{\rm h}}}{\frac{1}{T_{\rm m}}\frac{\mathrm{d}T_{\rm m}}{\mathrm{d}x}}=\frac{\frac{1}{\psi}\left[-\frac{\mathrm{Im}[-f_v]}{|1-f_v|^2}\times\frac{1}{|Z_{\rm N}|}-(\gamma-1)\,\mathrm{Im}\left[-f_k\right]\times|Z_{\rm N}|\right]+\mathrm{Re}\left[\frac{f_k-f_v}{(1-f_v)(1-\sigma)}\,\mathrm{e}^{-\mathrm{i}\varphi_Z}\right]}{\frac{-\psi}{|Z_{\rm N}||1-f_v|^2(1-\sigma^2)(\gamma-1)}\,\mathrm{Im}\left(f_k+\sigma\tilde{f}_v\right)+\mathrm{Re}\left[\frac{f_k-\tilde{f}_v}{(1+\sigma)(1-\tilde{f}_v)}\,\mathrm{e}^{\mathrm{i}\varphi_Z}\right]}.\tag{15}$$

2.4. Second law coefficient-of-performance of the TAC

The first law coefficient of performance COP_1 divided by the Carnot coefficient of performance $\mathrm{COP}_{\rm c}$ equals the second law coefficient of performance COP_2, that is,

$$\mathrm{COP}_2=\mathrm{COP}_1/\mathrm{COP}_{\rm c}.\tag{16}$$

According to Eqs. (9), (13) and (16), it can be yielded

$$\mathrm{COP}_2=\frac{\frac{\dot{Q}_{\rm c}}{-\Delta\dot{E}_2}}{\frac{T_{\rm m}}{\Delta T_{\rm m}}}=\frac{\frac{\dot{Q}}{-\mathrm{d}\dot{E}_2/\mathrm{d}x}}{\frac{T_{\rm m}}{\mathrm{d}T_{\rm m}/\mathrm{d}x}}=\frac{\frac{\psi}{|Z_{\rm N}||1-f_v|^2(1-\sigma^2)(\gamma-1)}\,\mathrm{Im}\left(f_k+\sigma\tilde{f}_v\right)-\mathrm{Re}\left[\frac{f_k-\tilde{f}_v}{(1+\sigma)(1-\tilde{f}_v)}\,\mathrm{e}^{\mathrm{i}\varphi_Z}\right]}{\frac{1}{\psi}\left[\frac{\mathrm{Im}[-f_v]}{|1-f_v|^2}\times\frac{1}{|Z_{\rm N}|}+(\gamma-1)\,\mathrm{Im}\left[-f_k\right]\times|Z_{\rm N}|\right]-\mathrm{Re}\left[\frac{f_k-f_v}{(1-f_v)(1-\sigma)}\,\mathrm{e}^{-\mathrm{i}\varphi_Z}\right]}.\tag{17}$$

As shown in Eqs. (7), (8), (15), and (17), the thermoacoustic conversion efficiency is determined by six parameters: the working gas parameters γ and σ, the structural parameters ζ and ψ, and the acoustic field parameters $|Z_{\rm N}|$ and φ_Z.

Due to extracting the factor of ψ and ζ, the frequency does not exist in the efficiency formula. The effect of the frequency on the efficiency can be transformed into the effect of the normalized length of the regenerator on the efficiency. It can be controlled and offset manually, which means that thermoacoustic devices with different frequencies can perform the same efficiency by adjusting the radius dimensions in proportion to the axis dimension to keep ζ and ψ constant. This is significant to guide the miniaturization design of the thermoacoustic device.

For example, there is a high-efficiency thermoacoustic device with the length of l^1, the frequency of f^1 and the hydraulic radius of $r_{\rm h}^1$. For designing a miniature thermoacoustic device with the same efficiency, ζ and ψ should be kept constant in the structure designing. Consequently, according to the definitions of ζ and ψ, $r_{\rm h}^2$, l^1 and f^2 can be gotten as follows:

$$r_{\rm h}^1/r_{\rm h}^2=\sqrt{l^1/l^2}=\sqrt{f^2/f^1}.\tag{18}$$

3. Results and discussion

Under the condition of helium as the working gas and $|Z_N| = 10$, the second law efficiency of the engine η_2 and the second law coefficient of performance of cooler COP_2 are calculated within certain ranges of operation factor of regenerator ψ, relative hydraulic radius ζ and leading phase φ_Z.

3.1. Regenerator of TAE

In this section, the regenerator of the thermoacoustic prime mover is discussed. The case of $d\dot{E}_2/dx > 0$ is of significance, and elsewhere, the case of $d\dot{E}_2/dx \leq 0$ is neglected and assumed to be zero in the figures. According to Ref. [28], this section just discusses the acoustic field with $-90^\circ < \varphi_Z < 0$ in which region the TAE can gain a higher acoustic power and better efficiency.

Figure 1 shows η_2 as a function of ζ and ψ with different φ_Z. Furthermore, the maximum η_2, the optimal ζ and the optimal ψ with different φ_Z are summarized in Figs. 2 and 3. It can be found that the maximum $\eta_2 = 0.786$ operation occurs when $\zeta = 0.15$, $\psi = 42.1$ and $\varphi_Z = -9^\circ$.

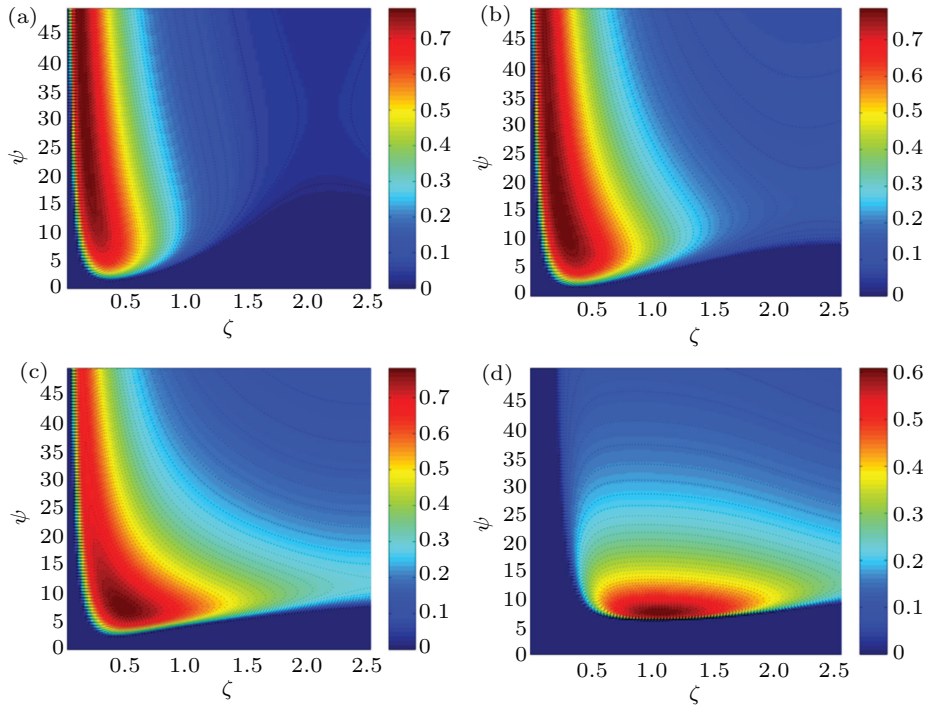


Fig. 1. The effect of ζ, ψ and different φ_Z on η_2: (a) $\varphi_Z = 0^\circ$, (b) $\varphi_Z = -30^\circ$, (c) $\varphi_Z = -60^\circ$, (d) $\varphi_Z = -90^\circ$.

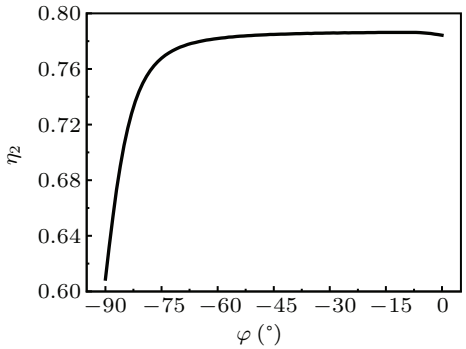


Fig. 2. The maximum η_2 with different φ_Z.

As shown in Fig. 2, the maximum η_2 does not appear at $\varphi_Z = 0^\circ$, but at $\varphi_Z = -9^\circ$. When gas works at the leading phase $\varphi_Z = 0^\circ$, the regenerator achieves the reversible thermoacoustic conversion in theory. The reversible thermoacoustic conversion can be realized by the reversible thermal contact which requires an infinitesimal hydraulic radius of the regenerator. However, this will lead to infinite viscous dissipation which will weaken the thermoacoustic gain and efficiency. So the finite hydraulic radius is adopted in the real traveling wave device, which makes the oscillating temperature of gas parcels lag the oscillating displacement. It indicates that the phase difference between the oscillating temperature and the oscillating pressure deviates from 90° because of the thermo-relaxation. Under such condition, for improving the thermoacoustic efficiency and gain, $\varphi_Z = -9^\circ \neq 0^\circ$ is of significance to match the phase deviation resulted by the thermo-relaxation.

As shown in Fig. 3, as φ_Z increases from -90° to 0°, the optimal ψ increases, and thus the optimal length of regenerator decreases because of $l_N \propto 1/\psi$ as shown in Eq. (11). It indicates that the optimal regenerator length of the standing wave engine is longer than that of the traveling wave engine. This property can explain the different lengths of the regenerators in the cascade TAE designed by Swift.[13] In 2003, Swift designed a cascade thermoacoustic engine consisting of three stages, and the lengths of the regenerator were 0.26 m, 0.031 m and 0.042 m, separately. It indicates that the regenerator length of the first stage is much larger than those of the second stage

and the third stage, because the first stage works in the standing wave field while the other two stages work in the traveling wave field.

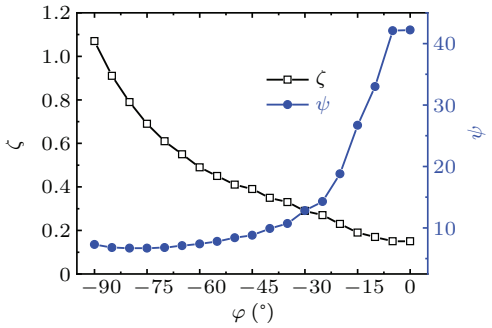


Fig. 3. The optimal ζ and the optimal ψ for the maximum η_2 versus φ_Z.

Sometimes, the thermoacoustic engine has been designed without optimizing the regenerator operation factor, while the regenerator operation factor could be important in the running process. According to Eq. (11), ψ is determined not only by the structure dimension (e.g., l_N), but also the operation parameter (e.g., T_h). We can choose the appropriate operation parameter T_h to adjust ψ. For example, there is a standing wave engine with the normalized length of $l_N = 0.025$. As shown in Fig. 3, the optimal ψ equals to 7.3. According to Eq. (11), we can choose the hot side temperature $T_h \approx T_c \frac{1+\pi\psi l_N}{1-\pi\psi l_N} = 665$ K to adjust ψ to its optimization, when the ambient side temperature $T_c \approx 300$ K is assumed.

3.2. Regenerator of TAC

This section focuses the discussion on the regenerator of the TAC. The case of $\dot{Q} > 0$ is significant, and elsewhere, the case of $\dot{Q} \leq 0$ is neglected and to be assumed as zero in the figures. According to Ref. [19], this section just discusses the acoustic field with $-180° < \varphi_Z < -90°$ in which the TAC can gain a higher cooling power and coefficient of performance.

Figure 4 shows the variation of COP_2 with various ζ, ψ and φ_Z. Furthermore, the maximum COP_2, the optimal ζ and the optimal ψ with different φ_Z are summarized in Figs. 5 and 6. It is quite obvious that the maximum $COP_2 = 0.786$ operation occurs when $\zeta = 0.17$, $\psi = 25.9$ and $\varphi_Z = -169°$.

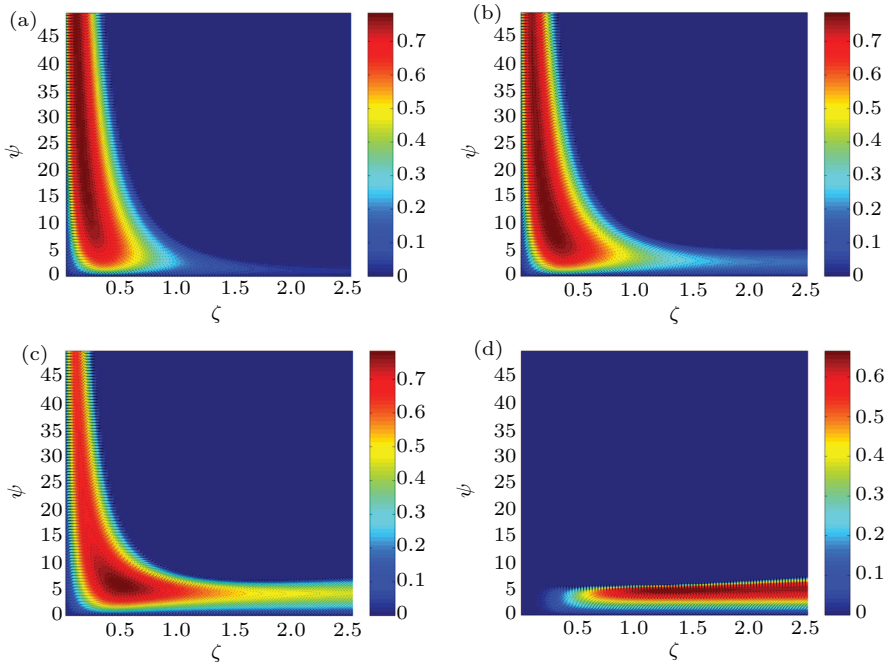


Fig. 4. The effect of ζ, ψ and φ_Z on COP_2: (a) $\varphi_Z = -180°$, (b) $\varphi_Z = -150°$, (c) $\varphi_Z = -120°$, (d) $\varphi_Z = -90°$.

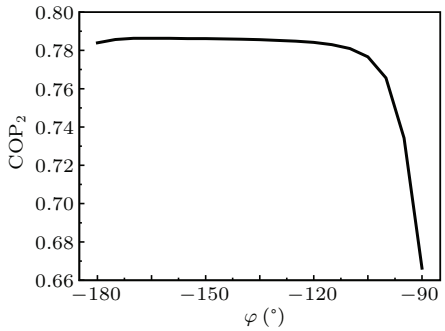


Fig. 5. The maximum COP_2 with different φ_Z.

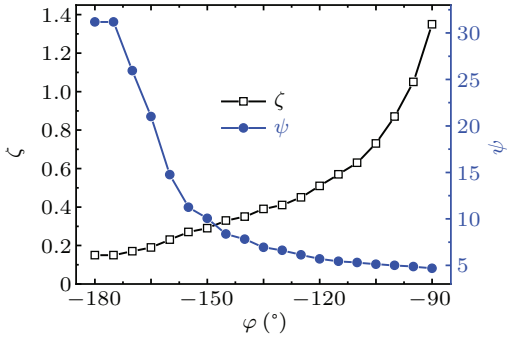


Fig. 6. The optimal ζ and the optimal ψ for the maximum COP_2 versus φ_Z.

As shown in Fig. 5, the maximum COP_2 does not appear at $\varphi_Z = -180°$, but at $\varphi_Z = -169°$. Similarly to the phenomenon that appears in η_2 optimization, the finite hydraulic radius value $\zeta = 0.17$ is accepted due to the viscous dissipation, and then $\varphi_Z = -169° \neq -180°$ is important to match the phase deviation because of the thermo-relaxation.

As shown in Fig. 6, with φ_Z increasing from $-180°$ to $-90°$, the optimal ψ decreases, and thus the optimal length of regenerator increases because of $l_N \propto 1/\psi$ as shown in Eq. (11). It indicates that the optimal regenerator length of the standing wave cooler is longer than that of the traveling wave cooler.

4. Conclusions

Based on the linear thermoacoustic theory, this paper extracts a normalized parameter named the regenerator operation factor, and then synthetically optimizes the dimension of the thermoacoustic regenerator by combining the regenerator operation factor, relative hydraulic radius and acoustic field parameter.

1) Due to extracting the regenerator operation factor and relative hydraulic radius, it is found that the influence of the frequency on the efficiency can be controlled and offset. Thermoacoustic devices with different frequencies can perform the same efficiency by adjusting the radius dimensions in proportion to the axis dimension. This is of significance to guide the miniaturization design of the thermoacoustic device.

2) The parameters relative to the regenerator length appear in the basal thermoacoustic formulas by extracting and analyzing the regenerator operation factor. It can help us optimize the length of the regenerator more easily, and control the temperature more effectively in the running process.

3) As the leading phase deviates from the traveling wave phase to the standing wave phase, the optimal length of the regenerator increases. It indicates that the optimal regenerator length of the standing wave device is longer than that of the traveling wave device.

4) Under the condition of helium as the working gas and $|Z_N| = 10$, the maximum second law efficiency of engine $\eta_2 = 0.786$ operation happens when $\zeta = 0.15$, $\psi = 42.1$ and $\varphi_Z = -9° \neq 0°$ because of the thermo-relaxation. The maximum second law coefficient of performance of cooler $COP_2 = 0.786$ operation happens when $\zeta = 0.17$, $\psi = 25.9$ and $\varphi_Z = -169°$ because of the thermo-relaxation.

5) The finite hydraulic radius is selected because of viscous dissipation, and the optimization of the leading phase is not the traveling phase because of the thermo-relaxation.

Acknowledgement

Project supported by the National Natural Science Foundation of China (Grant No. 51925605).

References

[1] Saechan P and Dhuchakallaya I 2020 *Energy Rep.* **6** 1456
[2] Ramadan I A, Bailliet H, Poignand G and Gardner D 2021 *Appl. Therm. Eng.* **189** 116705
[3] Carter R L, White M and Steele A M 1962 *Private communication of Atomics International Division of North American Aviation* **24** 458
[4] Sondhauss C 1850 *Ann. Phys.* **155** 1
[5] Ceperley P H 1979 *Acoust. Soc. Am.* **66** 1508
[6] Rott N 1980 *Adv. Appl. Mech.* **20** 135
[7] Swift G W 1988 *Acoust. Soc. Am.* **84** 1145
[8] Tijani M E H, Zeegers J C H and Waele T A M 2002 *Cryogenics* **42** 49
[9] Yu Z B, Li Q, Chen X, Guo F Z and Xie X J 2005 *Cryogenics* **45** 566
[10] Raspet R, Brewster J and Bass H E 1998 *Acoust. Soc. Am.* **103** 2395
[11] Tijani M E H, Zeegers J C H and Waele T A M 2002 *Acoust. Soc. Am.* **112** 134
[12] Kuzuu K and Hasegawa S 2021 *Appl. Therm. Eng.* **183** 116223
[13] Backhaus S and Swift G W 1999 *Nature* **399** 335
[14] Tsuda K and Ueda Y 2017 *Appl. Energy* **196** 62
[15] Yang R, Wang Y, Feng Y, Jin T and Tang K 2019 *Appl. Therm. Eng.* **148** 516
[16] Tan J, Wei J and Jin T 2019 *Appl. Therm. Eng.* **160** 114086
[17] Xu J Y, Luo E C and Hochgreb S 2020 *Appl. Energy* **271** 115167
[18] Rogozinski K, Nowak I and Nowak G 2017 *Energy* **138** 249
[19] Yang R, Meir A and Ramon G Z 2020 *Appl. Energy* **261** 114377
[20] Liu L, Liu Y and Duan F 2020 *Energy Convers. Manage.* **224** 113367
[21] Rahman A A and Zhang X 2019 *Int. J. Refrig.* **98** 35
[22] Xu J, Luo E and Hochgreb S 2020 *Appl. Energy* **271** 115167
[23] Wang X, Wu Z, Zhang L, Hu J and Luo E 2020 *Int. J. Refrig.* **120** 90
[24] Alamir M A 2020 *Therm. Sci. Eng. Prog.* **17** 100361
[25] Peng Y H, Feng H Y and Mao X A 2018 *Int. J. Refrig* **92** 246
[26] Shen C and He Y L 2009 *Appl. Therm. Eng.* **19** 2745
[27] Swift G W 2001 *Thermoacoustics* (New Mexico: Springer International Publishing) pp. 55–73
[28] Kang H F and Li Q 2010 *Cryogenics* **50** 450